
This is an electronic reprint of the original article.
This reprint may differ from the original in pagination and typographic detail.

Viitala, Raine; Widmaier, Thomas; Kuosmanen, Petri

Subcritical vibrations of a large flexible rotor efficiently reduced by modifying the bearing inner ring roundness profile

Published in:
Mechanical Systems and Signal Processing

DOI:
[10.1016/j.ymssp.2018.03.010](https://doi.org/10.1016/j.ymssp.2018.03.010)

Published: 15/09/2018

Document Version
Publisher's PDF, also known as Version of record

Published under the following license:
CC BY

Please cite the original version:
Viitala, R., Widmaier, T., & Kuosmanen, P. (2018). Subcritical vibrations of a large flexible rotor efficiently reduced by modifying the bearing inner ring roundness profile. *Mechanical Systems and Signal Processing*, 110, 42-58. <https://doi.org/10.1016/j.ymssp.2018.03.010>

This material is protected by copyright and other intellectual property rights, and duplication or sale of all or part of any of the repository collections is not permitted, except that material may be duplicated by you for your research use or educational purposes in electronic or print form. You must obtain permission for any other use. Electronic or print copies may not be offered, whether for sale or otherwise to anyone who is not an authorised user.



Subcritical vibrations of a large flexible rotor efficiently reduced by modifying the bearing inner ring roundness profile



Raine Viitala*, Thomas Widmaier, Petri Kuosmanen

Aalto University, School of Engineering, Department of Mechanical Engineering, Finland

ARTICLE INFO

Article history:

Received 24 August 2017

Received in revised form 28 February 2018

Accepted 5 March 2018

Keywords:

Rotor dynamics

Dynamic run-out

Low-order bearing waviness

Four-point method

ABSTRACT

Undesired vibration of a rotor is harmful for industrial processes and decreases the machine lifetime. In industrial processes, large rotors are commonly operated below the critical speed.

In the subcritical speed range, the bearings are an important excitation source of vibration. The bearing inner ring based excitation is observed at a frequency, which is the rotor rotating frequency multiplied by the number of undulations in the roundness profile of the roller race of the bearing inner ring. Subcritical resonance occurs, when the bearing excitation frequency equals the natural frequency of the rotor system.

The present study investigates the effect of the bearing inner ring roundness profile on the subcritical vibrations of a flexible rotor. The roundness profile of the bearing inner ring was measured, while installed on the rotor shaft. The roundness profile was modified to five different geometries to investigate different excitation cases. Finally, the roundness error of the inner ring was minimized.

The rotor subcritical vibration was measured with each bearing inner ring geometry in the horizontal and vertical directions. The analysis was focused on the 2nd, 3rd and 4th harmonic vibration components, occurring at 1/2, 1/3 and 1/4 of the critical rotational speed.

The results clearly suggest that the roundness profile of the roller race of the bearing inner ring affects the rotor subcritical vibration significantly. The increased waviness components of the bearing inner ring roundness profile increased the corresponding subcritical vibration amplitude. Minimizing the roundness error decreased the subcritical vibration substantially.

© 2018 The Author(s). Published by Elsevier Ltd. This is an open access article under the CC BY license (<http://creativecommons.org/licenses/by/4.0/>).

1. Introduction

Rotor running accuracy is a critical factor in a rotor system. The vibration levels exhibited by the rotor and transmitted to the bearings and other suspending components of the rotor foundation can reduce the lifetime of the apparatus and can increase the production downtime, with both leading to avoidable costs. Rotor balancing is a commonly used method in the industry for reducing vibration derived from static and dynamic unbalance [1]. Furthermore, optimizing the bearing inner ring geometry may also improve the vibrational situation by reducing the excitation from the rotor bearings.

* Corresponding author at: Aalto University, School of Engineering, Dept. of Mechanical Engineering, Engineering Design, Sähkötieteenkatu 4P, PL 14400, 00076 Aalto, Finland.

E-mail address: raine.viitala@aalto.fi (R. Viitala).

Nomenclature

c.	circa, approximately
CNC	Computer Numeric Control
DAQ	Data Acquisition
f	frequency [Hz]
f_i	inner ring excitation frequency [Hz]
FEM	Finite Element Method
FFT	Fast Fourier Transform
H	harmonic
k	waviness component/lobe number
LPF	Low Pass Filter
N	positive integer, $N \geq 2$
p	positive integer
PCI	Peripheral Component Interconnect
q	positive integer
RC	resistor-capacitor
$S_1 \dots S_4$	four-point method sensors
TTL	transistor-transistor logic
u	number of rolling elements
U	uncertainty
ω_i	angular frequency of the inner ring [Hz]
ω_c	angular frequency of the cage [Hz]

The flexible rotor subcritical behaviour is important, e.g., in industry fields using electric motors and generators and turbines. The rotor assemblies are typically designed to operate on a certain speed range. The excitation from the bearing inner ring is dependent on the rotating frequency of the rotor and the waviness number (number of undulations) of the roller raceway surface. One undulation per revolution excites the rotor at its own rotating frequency; resonance and thus increased vibration is apparent when the rotor speed approaches its natural frequency. Moreover, two undulations per revolution excite the rotor at twice the frequency of the rotor itself, which leads to resonance at a rotor speed half the natural frequency. These superharmonic bearing excitations produce resonance peaks also on the subcritical (below natural frequency) speed range and are likely to occur when the ratio between the natural frequency and the running frequency is a positive integer.

The actual rotor run-out during operation is relevant in certain fields of industry such as papermaking, which utilizes the rotor (roll) surface to form the end product. The roll surface movement towards the paper web direction (run-out) is critical considering the product quality. The roll surface movement is transferred to the product and observed as undesired, periodic thickness variation. Roll surface geometry can be optimized using, for example, a roll surface measurement and grinding method proposed by Kuosmanen [2]. In addition, improving the bearing assembly may also have a significant effect on the roll run-out in operationally important directions, such as nip direction.

The design speed for a large, flexible rotor is usually below the critical speed, i.e., natural frequency of the rotor. Some rotors are designed to operate in a wide speed range covering the frequencies $1/2, 1/3, 1/4 \dots 1/N$ times the natural frequency. In this range, the bearing inner ring raceway profile is one of the reasons for superharmonic excitation causing subharmonic vibrations.

The early studies concerning the waviness of the bearing inner ring was conducted by Gustafsson et al. [3] and Yhland [4]. They found in their experimental studies that the lobe number (number of waves) multiplied by the inner ring angular velocity dominates the vibration spectrum as proposed also by Slocum [5]. Aktürk [6] confirmed similar results with his mathematical model of waviness in bearing elements with balls as the rolling elements. Excitation caused by a defected inner ring (small crack) was analysed with a similar model by Arslan and Aktürk [7].

The connection between the waviness of the inner ring and the radial vibrations is expressed with the following connection [3,4,6]: the inner ring waviness of the orders

$$k = q \cdot u \pm p \quad (1)$$

causes vibration at frequencies

$$f = q \cdot u (\omega_i - \omega_c) \pm p \cdot \omega_i, \quad (2)$$

where $q \geq 0$ and $p \geq 1$ are positive integers, u is the number of rolling elements, ω_i is the angular frequency of the inner ring and ω_c is the angular frequency of the cage holding the rolling elements. When q is set to zero, the rotor angular frequencies producing harmonic resonance vibration are found, when the Eq. (2) gives the natural frequency of the rotor.

A dynamic bearing excitation model including Hertzian contact forces between the bearing elements has been proposed by Changqing et al. [8]. However, the investigated waviness number was as high as 18. Harsha et al. [9–13] have developed a

similar model. Their research confirms the Eqs. (1) and (2) also using dynamic models utilizing the rotor interaction. The waviness numbers were higher than 5 and more interest is expressed towards the excitation caused by the ball passage frequency ($\omega_i - \omega_c$). The ball passage frequency based excitations are more important in cases in which the number of bearing elements is close to the dominating waviness number. In a related approach, Jang and Jeong [14] added the centrifugal forces and the gyroscopic moment of the ball to the model. However, the research was again limited to waviness numbers higher than 15.

A dynamic six degrees of freedom model of a rigid rotor is included in a simulation model by Babu et al. [15]. The results are validated with experimental measurements. In this research also, the waviness number orders (6, 15 and 25) are too high to be considered in the case of subcritical vibration of flexible rotors. However, the results agree with Eqs. (1) and (2).

Shah et al. [16] conducted a study considering local defects in the bearing inner and outer rings. The waviness component of order 7 was included. The results confirmed Eqs. (1) and (2).

Liu et al. [17] conducted vibration measurements of a ball bearing. In addition, the waviness of the inner and outer race of the bearing was measured. It was found that the waviness has the most important influence on vibration at the natural frequency of the system.

Sopanen and Mikkola [18,19] built a simulation model using a commercially available multi-body system software MSC ADAMS. The model included an elastic ball bearing model utilizing the mathematical properties of the software. A flexible rotor supported by the bearings was introduced. The effect of the inner ring waviness of orders 2, 3, 4 and 5 on the rotor response was studied. A similar waviness profile (similar amplitudes and phase angles) consisting of the specific waviness components is emulated by both of the bearings supporting the rotor. Significant subharmonic resonances are observed at angular velocities 1/2, 1/3, 1/4, 1/5 times the natural frequency. The authors suggest that the resonances are evidently caused by the waviness of the inner rings of the bearings. The authors state that these subharmonic resonances may be harmful if the rotor is designed to operate under the critical speed. However, the excitation is considered to be weaker if the phase angles of the waviness profiles of the two bearings differ from each other.

Ghahamchi et al. [20] have developed a dynamic simulation model of a spherical roller bearing instead of a ball bearing. The model includes Hertzian contact forces with elastic deformation under loads. In addition, a rotor system with a rigid rotor supported by two similar bearings is presented. The waviness of the roller paths can be added to the model. A similar spherical roller bearing model, which included the waviness of the bearing inner and outer rings, was used by Heikkinen [21]. The waviness components were measured and emulated in the simulation model. In addition, a large flexible rotor (paper machine roll) was modelled with FEM (finite element method) and included into the model. The response of the rotor was simulated with the bearing model and compared against measurement results. The simulation model was able to detect the 2nd harmonic resonance frequency accurately in both horizontal and vertical directions. Other harmonic resonance components were also detected. However, their frequencies deviated from the measured results. Additionally, the 2nd harmonic resonance amplitude, especially in the vertical direction, was simulated to be threefold compared to the measurement. The imperfections of the model were supposed to result from the stiffness description of the foundation.

In addition, a paper published by partly the same authors as the present study [22] focuses on the simulation approach in investigating the subcritical vibration of large rotors, but the results are compared against experimental tests as well. The simulation model included the lower order waviness of the bearing inner ring. The effect of bearing waviness of order 2 on the 2nd harmonic subcritical vibration resonance amplitude was clearly detected by the simulation model and the reference measurements. The frequency of the 2nd harmonic subcritical vibration was detected fairly accurately by the simulation model. However, the simulated resonance amplitude was substantially deviated from the measured amplitude. The effect of waviness of orders 3 and 4 on the subcritical vibration could be detected as well. A comparison was made between mathematically round bearings without any out-of-roundness and bearings emulating the bearing geometry in the reference measurement equipment. The bearings emulating the actual bearing geometry produced substantially higher 2nd harmonic subcritical vibration confirming the importance of the waviness components of the bearing inner ring roundness profile. The 2nd order waviness had the highest amplitude in the actual bearings.

Although researchers have focused on the effect of bearing geometry errors, a profound empirical study of the effect of the lower order waviness components of the bearing inner ring roundness profile on the vibration of a large and flexible rotor is lacking. The closest approaches to this context are made by Sopanen and Mikkola [18,19], Ghahamchi et al. [20] and Heikkinen [21], who all proposed simulation methods appropriate for investigating excitations from bearing inner ring lower order waviness. The present study improves the state-of-the-art through an experimental test series with an industrial-scale test rotor and several different roundness profiles of the bearing inner ring, featuring different distributions of waviness.

The present study investigates the connection between the waviness components of the spherical roller bearing inner ring assembled on the rotor shaft and the subcritical harmonic resonance vibration of a large rotor. Moreover, the study focuses on the low order waviness components from two to four undulations per revolution, which cause excitation at frequencies two, three and four times the rotating frequency of the rotor. When these excitations coincide with the natural frequency of the rotor system, a resonance vibration is established. Consequently, these excitations induce harmonic vibration resonance at rotor angular frequencies 1/2, 1/3, 1/4 multiplied by the natural frequency. In practice, the desired waviness component of the bearing inner ring was amplified through inserting thin steel strips between the conical adapter sleeve of the bearing and the installation shaft. The dynamic response of the rotor was measured and analysed with each different roundness profile concentrating on the subcritical vibration frequencies. Finally, all the waviness components were

minimized using the same steel strip deformation technique, leading to minimized roundness error of the installed bearing inner ring as well.

The study focuses on experimental research to validate the results produced earlier by other researchers and to ensure the utility with industrial large-scale rotors as well.

2. Methods

2.1. Rotor dynamic response measurement

A paper machine roll was used as a test rotor. The rotor response was measured utilizing the four-point method [23] by extracting the rotor central axis movement at each measured speed and at each measured cross-section. The four-point method was chosen to separate the roll roundness profile from the roll central axis movement in a reliable way.

2.1.1. Equipment

The rotor dynamic measurement setup was built on a CNC-controlled (computer numerically controlled) roll grinding machine. The grinding machine was used to control the roll rotating speed, and to move the sensor holder frame to different cross sections. The bearing housings were installed on steel stands fixed on a concrete machine bed. The roll was connected to the drive unit with an aligned universal joint to prevent excitations resulting from sinusoidal angular velocity variation. Fig. 1 presents the setup in the laboratory.

In Fig. 2, the main dimensions of the test rotor are presented in millimetres. In addition, the measured cross-sections are displayed and numbered from 1 to 5.

2.1.2. Sensors

To collect the roll dynamic run-out data for the four-point method, four laser sensors were used (Fig. 3). The high surface velocity prevents the usage of tactile sensors due to vibration, sensor head bouncing and friction leading to excessive



Fig. 1. Rotor dynamic response measurement setup built on a roll grinding machine.

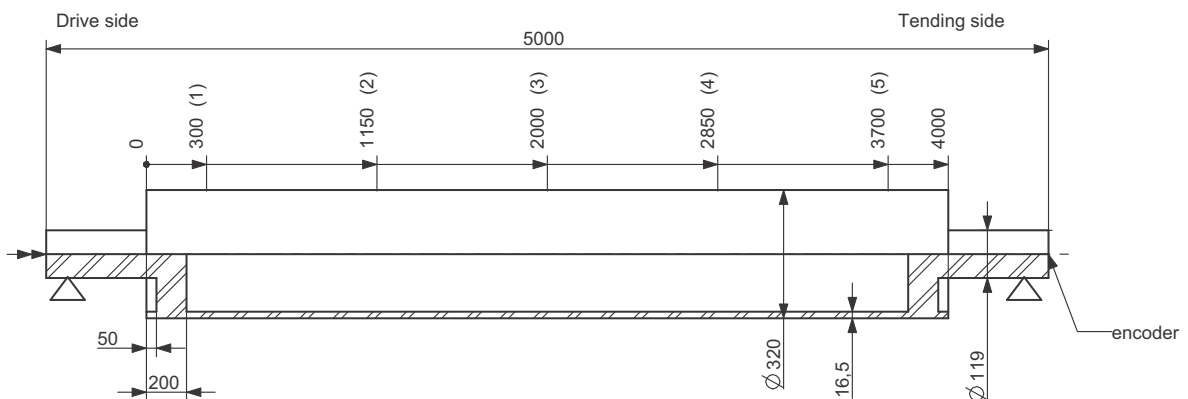


Fig. 2. Main dimensions of the rotor and measured cross-sections from 1 to 5.

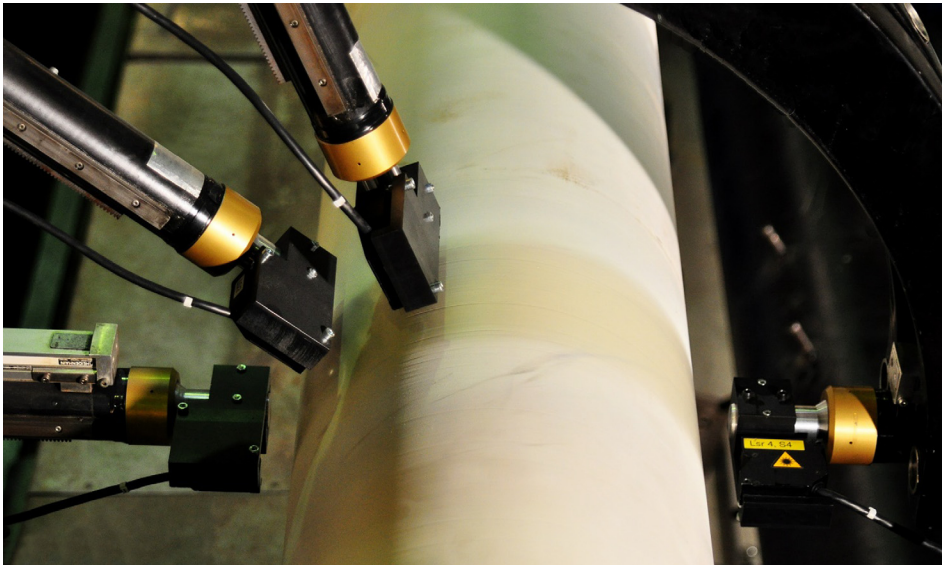


Fig. 3. The four-point method applied to roll dynamic response measurement with laser sensors.

warming-up. The laser sensors were triangulation reflective laser sensors (Matsushita NAIS LM 300). The roll surface was painted with an optimal colour at the measurement cross-sections to ensure exact reflection. The varying thickness of the paint layer did not affect the measurement results, since the four-point method was used to detect the central axis movement. Laser sensor displacements were converted to voltages (1 V corresponds to 1 mm) with an amplifier.

The angular position of the roll was measured with an incremental rotary encoder (Heidenhain ROD 420 with 1024 pulses/revolution). The encoder reference pulse also triggered the measurement task to enable an absolute measurement of the roll angle.

2.1.3. Data acquisition and analysis

A data acquisition system was developed on a National Instruments USB-6215 data acquisition card. The card contains 16-bit analog inputs for voltages in range from -10 to $+10$ V. The maximum sample rate is 250 kS/s, which indicates that each channel for the four measured displacements has a maximum rate of 62.5 kS/s when the multiplexing function of the card is considered. The measurement task was programmed into the card using LabVIEW.

Encoder reference and pulse train signals were used as a trigger and an external sampling clock. Both the differential signals were conditioned with a differential line receiver (Texas Instruments SN75175), which transmits the single-ended pulses to the data acquisition card.

The analog voltages produced by the laser displacement sensor amplifiers were low-pass filtered to prevent aliasing. The low-pass filter was a two-stage RC-filter with a cut-off frequency of 1940 Hz. Since the encoder was connected rigidly to the roll, the actual sample rate varied during the measurement due to the varying roll speed. The roll rotational frequency range from 4 Hz to 18 Hz results in corresponding data acquisition frequencies from 4096 Hz to 18432 Hz when 1024 samples are collected during each revolution. Even the lowest measurement frequency exceeded twice the low-pass filter cut-off frequency, which ensured a correct anti-aliasing operation.

An encoder was used as an external clock to achieve an accurate synchronous averaging [24]. Synchronous averaging is used to enhance the quality of a measured signal when the measured system has reached a steady state, and when collecting the data during multiple similar cycles of the system is possible.

Generally, this signal processing method is applied to periodic signals, such as the vibration of rotating machinery [25]. The original method uses a trigger signal, which is phase locked with the rotating component of interest, to distinguish between the periods of the important signal [24,26]. Hochmann and Sadok [27] suggest improving the method further by using an external phase locked clock signal for measurement timing, which was used in the present study.

In the rotor dynamic response measurements, synchronous averaging with an external measurement clock was utilized. The encoder reference pulse triggered the measurement, after which the encoder TTL-level (transistor-transistor logic) square wave pulse train of 1024 pulses/revolution was used as a measurement clock. Consequently, this indicated that 1024 samples were collected at the same angular position in every revolution. The measurement consisted of samples acquired during 100 revolutions of the roll. Finally, synchronous averaging was applied to the digitized samples: 100 samples at equal angular positions were averaged to achieve the final estimate of the dynamic run-out at each of the 1024 angular positions.

The four-point method [23,28] algorithm was applied to the measured data after the data acquisition and synchronous averaging. The main advantage of the method is the ability to separate the motion of the rotating axis and the roundness of the cross-section from each other. Traditional roundness measurement devices cannot be used because of the large size of the measured objects. The four-point method merges a two-point diameter measurement method and the Ozono three-point method [29]. Fig. 4 presents the measurement setup and the sensor orientations in each method.

Finally, the centre axis movement data provided by the four-point algorithm was analysed with Matlab using FFT (Fast Fourier Transform) to reveal the harmonic components of the roll response.

The following procedure, presented also in Fig. 5, was applied to the measurement data acquisition and analysis:

1. An encoder was used as a trigger and an external clock.
2. Laser sensor voltages were low-pass filtered to prevent aliasing.
3. 100 revolutions of dynamic run-out data was acquired with a data acquisition card (DAQ).
4. Data was transmitted to a PC.
5. 100 revolutions of data were synchronously averaged.
6. The four-point algorithm was applied.
7. The central axis movement was analysed with FFT in MATLAB.

2.2. Bearing inner ring geometry measurement

The rotor was supported by two spherical roller bearings (SKF 23124 CCK/W33). The bearing was installed on the rotor shaft with a conical adapter sleeve (H 3124). The bearing contains roller elements in two rows. Fig. 6 presents the elements and dimensions of the bearing.

The bearing was tightened and fastened on the shaft using a conical adapter sleeve. The sleeve is pulled with a tightening nut, which pushes the bearing in the opposite direction simultaneously (Fig. 6). The correct tightness is achieved when the clearance between the rolling elements and the outer ring has reduced to a prescribed value. The clearance was measured with a feeler gauge. The clearance for this application was 0.06 mm, in accordance with the SKF bearing assembly instructions.

The geometry of the bearing inner ring was measured utilizing the four-point method, which enables the separation of the central axis movement and the bearing surface geometry. The bearing inner ring was installed on the rotor shaft during the measurement.

2.2.1. Equipment and sensors

The measurement set-up was built on the roll grinding machine introduced in Section 2.1.1. The roll bearing housings were disassembled and replaced with a different support, which made it possible to examine the bearings on the rotor shaft. The roll was connected to the drive unit through a drive shaft equipped with universal joints.

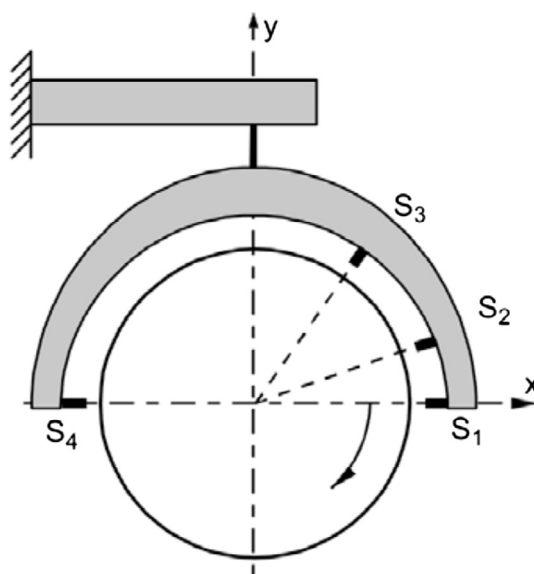


Fig. 4. Four-point method sensor orientations in relation to the measured object. In the two-point method, only sensors S1 and S4 are utilized. In the Ozono three-point method, sensor signals S1, S2 and S3 are used. The angles of the sensors starting from S1 are 0°, 38°, 67° and 180° [23].

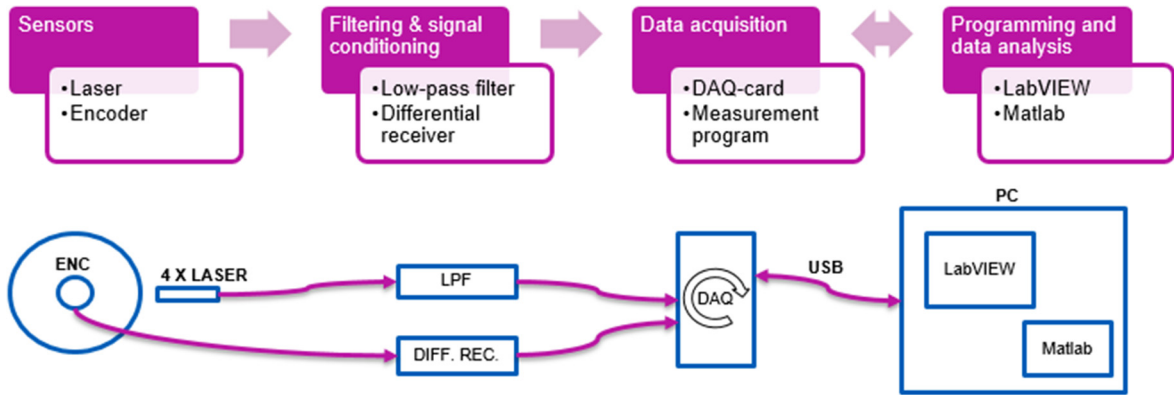


Fig. 5. Measurement procedure and data acquisition. LPF is low-pass filter and DIFF. REC is a differential line receiver.

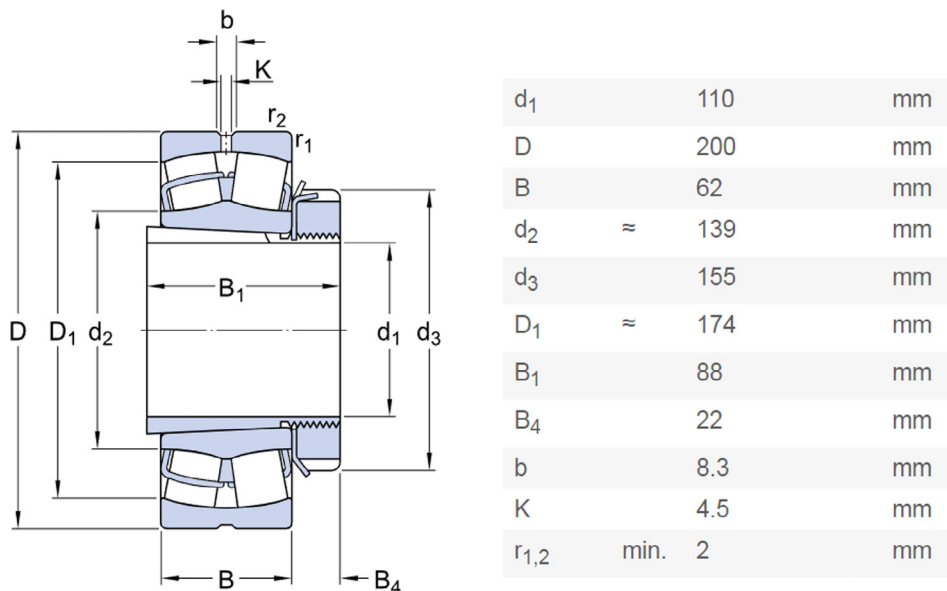


Fig. 6. Bearing SKF 23124 CCK/W33 equipped with a conical adapter sleeve H 3124 (SKF 2017).

The bearing outer ring and roller elements were disassembled while the inner ring was still installed on the rotor shaft. After the loosening of the tightening nut, the roller elements and their holder were removed in addition to the outer bearing ring. The bearing inner ring together with the conical adapter sleeve were left on the shaft.

The bearing inner ring measurement setup is presented in Fig. 7. The sensor holder arm was fastened to the grinding machine tool holder; the grinding machine was used to move the sensor arm to different measurement cross-sections. Four Heidenhain MT12 tactile sensors collected the static run-out data for the four-point method. An encoder recorded the phase angle of the roll and triggered the measurement.

The arrangement of the measured cross-sections is presented in Fig. 8. The 2nd and the 5th cross-section represent the middle cross-sections for both roller element rows. The cross-sections start in ascending order from the end of the roll. Fig. 8 reveals also the curved surface geometry of the roller element paths. To measure the roundness profile of a curved surface, principles dictated by ISO 1101 for conical surfaces were applied. The surface curvature leads to some unavoidable alignment errors of the sensor probe contact relative to the workpiece. The diameter of the probe ball-type contact was 3.2 mm. In practice, this implies that the sensor measurement direction is not the normal direction of the surface. However, the error was considered insignificant, since the emphasis was on the bearing geometry changes instead of absolute values.

2.2.2. Data acquisition and analysis

The static run-out signals produced by the Heidenhain MT12 tactile sensors were collected with a Heidenhain IK 220 evaluation electronics card. The evaluation electronics card supplied by the sensor manufacturer was responsible for all signal processing and finally the digitized values were available for reading.

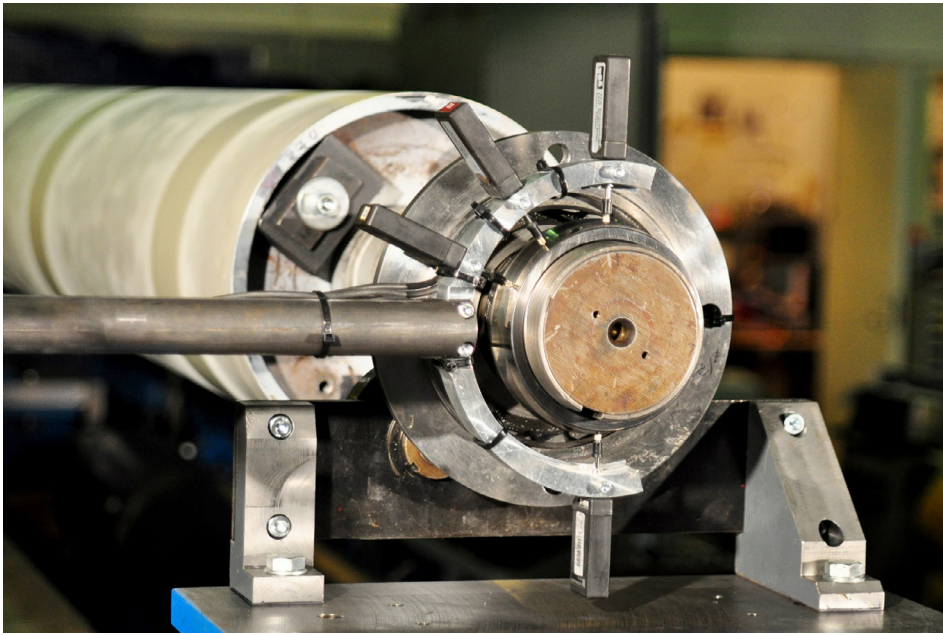


Fig. 7. Bearing inner ring measurement setup.

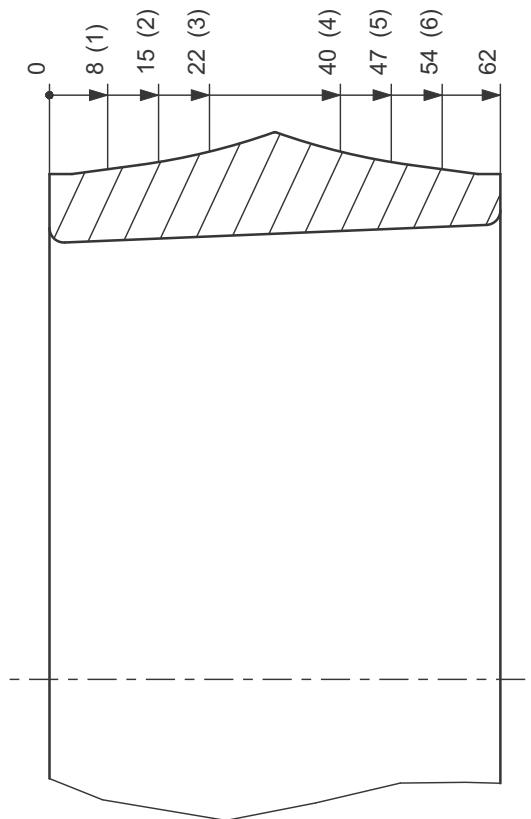


Fig. 8. Schematic of the measured cross-sections. The 2nd and the 5th cross-sections were chosen so that they were in the middle of the bearing roller path.

The encoder was used to trigger the measurement. The measurement principle was similar to the rotor dynamic measurement; the rotary encoder was used as an external measurement clock, which ensured acquisition of static run-out samples in equal bearing phase angles on every occasion. Moreover, the slightly varying angular velocity of the bearing does not affect the measurement accuracy when using external measurement clock, which is phase locked with the bearing.

After the sample acquisition, the four-point algorithm was applied to the collected samples. The bearing central axis movement was removed from the data. Finally, the bearing inner ring surface geometry profile was analysed with Fast Fourier transform to expose the waviness components of the bearing geometry.

The measurement procedure, presented also in Fig. 9, was as follows:

1. A rotary encoder was used as a trigger and a measurement clock.
2. Static run-out signals (one revolution) were acquired from MT 12 sensors.
3. IK 220 evaluation electronics digitized the signal values.
4. The four-point method was applied.
5. The bearing inner ring roundness profile was analysed with FFT in Matlab.

2.3. Deforming the bearing inner ring

The bearing inner ring was modified to investigate rotor dynamic behaviour with bearing inner rings of various different roundness profiles. In total, four different modifications to the roundness profile of the bearing inner ring were made; oval, triangular, quadrangular and minimum error.

Fig. 10 presents the first case (oval roundness profile, 2nd waviness component amplified), in which two steel strips were inserted between the conical sleeve and the shaft. The other forms were achieved utilizing a similar technique. In the last case, minimum roundness error, multiple steel strips were inserted between the conical sleeve and the shaft in different angular positions to reduce the roundness error. The thicknesses of the used steel strips were 0.01 mm, 0.02 mm and 0.03 mm. The desired shape was achieved using a trial-and-error method, i.e., the bearing inner ring was installed on the shaft after each modification and the obtained geometry was measured. The original shape of the bearing was used as an initial state to calculate the positions of the deforming strips.

The conical sleeve and the bearing inner ring were installed in the same angular position in relation to the rotor shaft throughout the research.

2.4. Experimental procedure

The following procedure was applied to investigate the connection between the bearing inner ring geometry and rotor vibration.

1. The roll centre point movement was measured in five sections in the roll rotating frequency range from 4 Hz to 18 Hz with 0.2 Hz rotating frequency increments.
2. The rotor centre point movement was analysed in frequency domain to discover the subcritical vibration components and their amplitudes.
3. The bearing outer ring and roller elements were disassembled and the inner ring roundness profile was measured in six sections at tending and initially also at the drive end.
4. The waviness components of the roundness profile were discovered through an analysis in the frequency domain.

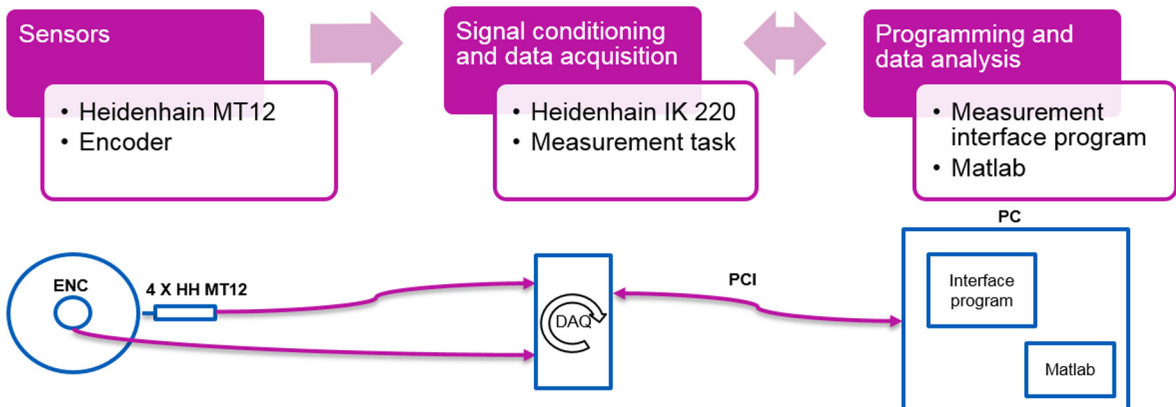


Fig. 9. Measurement procedure and data acquisition for the bearing geometry measurement.

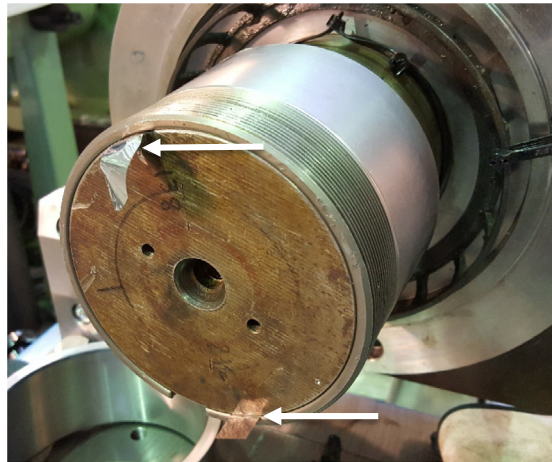


Fig. 10. Two steel strips inserted between the rotor shaft and the bearing conical adapter sleeve to achieve an oval form of the bearing inner ring.

5. The tending end inner ring was deformed with thin steel strips between the shaft and the conical adapter sleeve to amplify the ovality (2-lobe) of the bearing. The geometry achieved was verified before assembling the rest of the bearing.
6. Stages from 1 to 4 were repeated.
7. The inner ring was deformed again to amplify the triangular (3-lobe) shape of the bearing.
8. Stages from 1 to 4 were repeated.
9. The inner ring was deformed again to amplify the quadrangular (4-lobe) shape of the bearing.
10. Stages from 1 to 4 were repeated.
11. Based on the earlier deforming of the bearing inner ring and the measurement results, the bearing inner ring roundness error was minimized through inserting multiple steel strips between the shaft and the adapter sleeve in different angular positions.
12. Stages from 1 to 4 are repeated.

During the experimental research procedure, parts of the rotor assembly and bearing assembly had to be disassembled and reassembled multiple times. Particular care was taken to ensure the similar angular positions of the machine elements each time. This procedure enabled independent comparison of the influence of different bearing inner ring geometries.

3. Results

3.1. Bearing inner ring roundness profiles

Fig. 11 presents the roundness profiles of the installed bearing inner ring in five different cases. The waviness component amplitude distribution of orders from the 2nd to the 6th is presented in **Fig. 12**. The original roundness profile had a roundness value of 27.4 μm . The original geometry was dominated by the 2nd harmonic waviness, which equals to two lobes per revolution. In deformation cases 2–4 (oval, triangular, quadrangular), the eligible component dominated the roundness component distribution. However, the deformation method affected to other waviness components as well, e.g., the 4th harmonic was amplified substantially in the oval geometry. No substantial difference between the different measurement cross-sections (2nd and 5th) was observed. In addition, the roundness error was amplified in cases 2–4, the maximum being 55.5 μm in the oval profile. In the deformation case 5 (minimized roundness error) the roundness error was reduced to 10.4 μm . The roundness profile waviness components were reduced compared to the original geometry and none of them was observed to dominate the distribution.

3.2. Rotor subcritical vibration in different bearing deformation cases

The results from the rotor vibration at the middle cross-section (2000 mm, **Fig. 2**) are presented as frequency spectra in **Fig. 13**. The results represent the measurements in horizontal and vertical directions with five different tending side bearing inner ring roundness profiles. In addition, the resonance peak amplitudes in each case are collected into a bar chart (**Fig. 14**) for comparison purposes. In general, an increase in the corresponding harmonic vibration resonance peak amplitude was observed in each bearing deformation case. With minimized roundness error, the resonance peak amplitudes of all harmonic components reduced except for the 3rd harmonic in the vertical direction, which increased slightly.

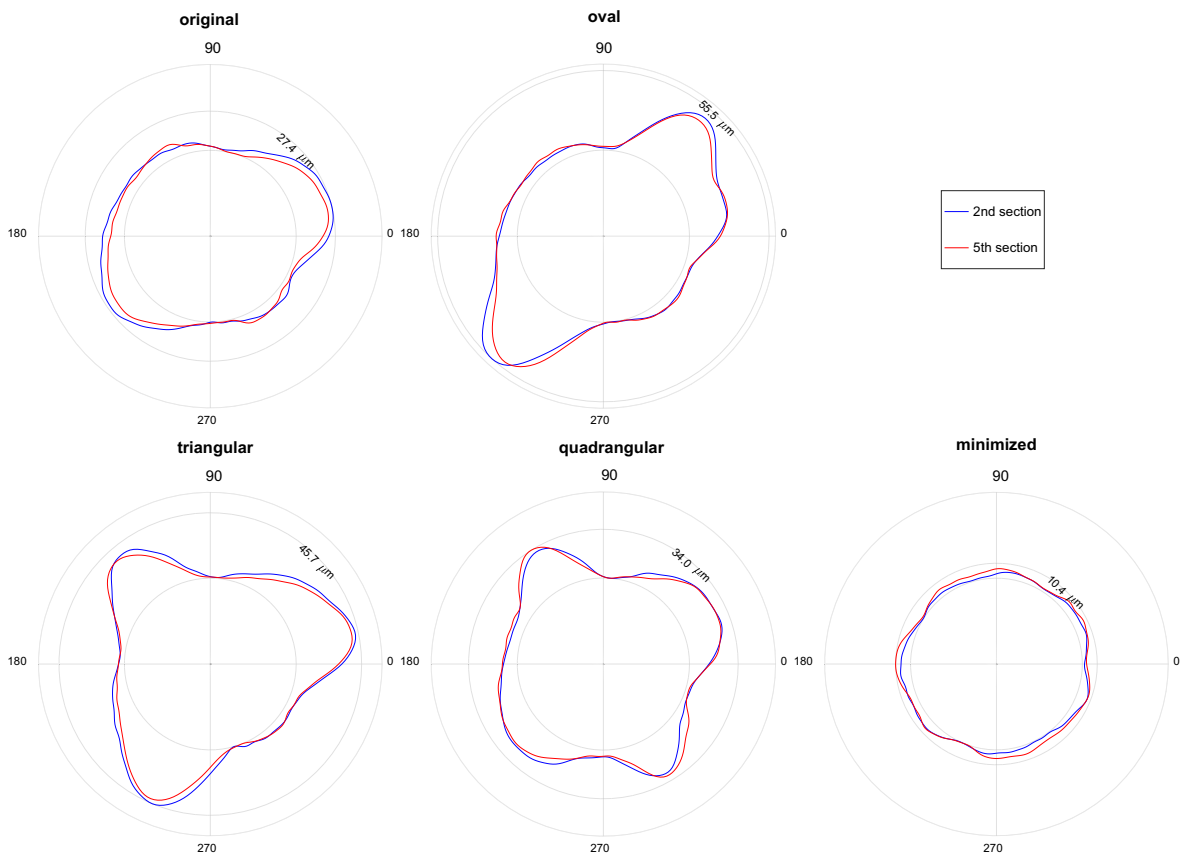


Fig. 11. Tending side bearing inner ring roundness profiles in five different cases. Only the profiles measured in the middle of both rolling element paths are presented (2nd and 5th section, Fig. 8). The roundness profile scale is the same in each case.

3.2.1. Original bearing inner ring roundness profile

The horizontal response was dominated by the 2nd harmonic component, the amplitude of which at resonance was 300 μm at the middle cross section. The 3rd and the 4th harmonic resonance amplitude was circa (c.) 60 μm . The rotating speed at which the resonance occurred suggests that the lowest bending mode natural frequency of the rotor system in the horizontal direction is c. 21.6 Hz ($2 \times 10.8 \text{ Hz} = 21.6 \text{ Hz}$, $3 \times 7.2 \text{ Hz} = 21.6 \text{ Hz}$, $4 \times 5.4 \text{ Hz} = 21.6 \text{ Hz}$).

The vertical rotational axis vibration movement resulted in lower resonance amplitudes and higher frequencies indicating a stiffer foundation in the vertical direction. Nevertheless, the 2nd harmonic vibration resonance peak was dominating also in the vertical direction. A small additional peak was observed at c. 11 Hz in the 2nd harmonic curve. In the vertical direction, the rotation speeds at which the resonance peaks occur suggest that the lowest bending mode natural frequency of the rotor system in the vertical direction is c. 30 Hz.

3.2.2. Oval bearing inner ring roundness profile

In the horizontal direction, the most significant change was in the 2nd harmonic component. Additionally, the 4th harmonic component amplitude at resonance increased substantially, although its absolute value was still limited compared to the dominating 2nd harmonic component.

In the vertical direction, similar results when compared to the horizontal direction were acquired in terms of the 2nd harmonic component: the peak amplitude was increased compared with the original setup. However, the 4th harmonic component decreased slightly, whereas in the horizontal direction it increased moderately. Also in this measurement, another smaller peak at the 2nd harmonic response curve was detected at the rotating frequency of c. 11 Hz, suggesting that the horizontal 2nd harmonic resonance has an effect on the vertical response.

3.2.3. Triangular bearing inner ring roundness profile

In the horizontal direction, a substantial increase in the 3rd harmonic resonance peak amplitude was noticed as well as minor increases in the 2nd and 4th harmonic components. The triangular case in Fig. 13 also shows more noisy harmonic response curves indicating that the excitation state was more complicated compared to previous cases.

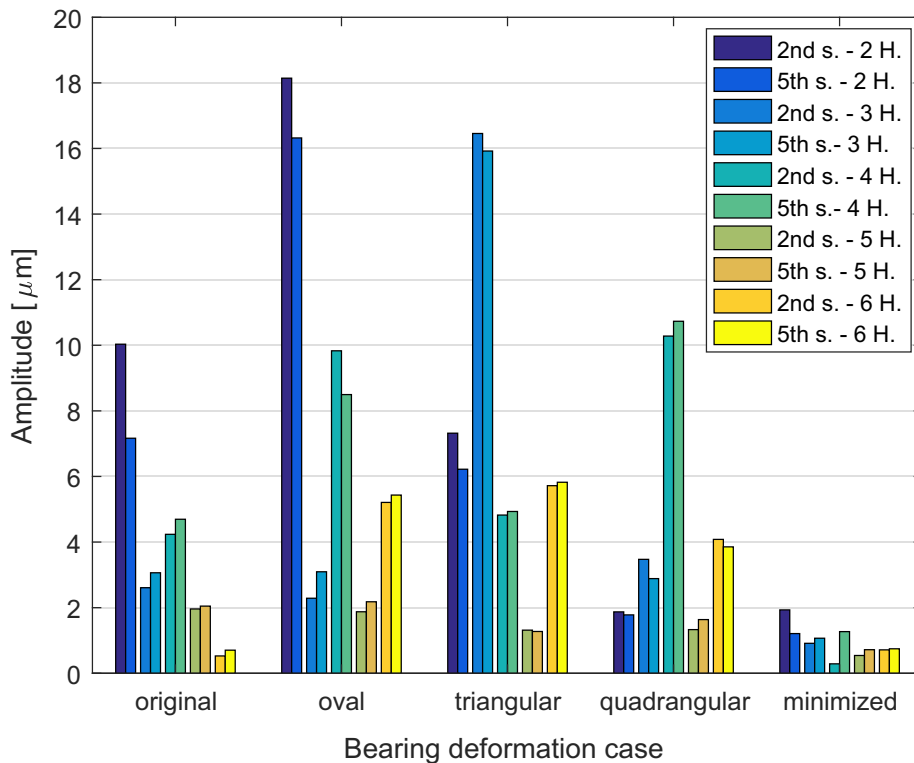


Fig. 12. The waviness component amplitudes of the bearing inner ring roundness profiles in five different cases. The different cases correspond to the roundness profiles presented in Fig. 11. Only the amplitudes in the middle of both rolling element paths are presented (2nd and 5th section, Fig. 8). 2H stands for the 2nd harmonic waviness component equal to two lobes per revolution etc.

In the vertical direction, a major increase in the vertical direction 3rd harmonic resonance peak amplitude was achieved compared to the original measurement setup. Furthermore, the amplitude of the 3rd harmonic component resonance peak exceeded the 2nd harmonic component peak amplitude, confirming the relevance of the 3rd harmonic component within the total vibrational behaviour. Moreover, an increase was observed in the 2nd and 4th harmonic components, the latter having more than a tenfold resonance peak increase.

3.2.4. Quadrangular bearing inner ring roundness profile

In the horizontal direction, the amplitude of the 4th harmonic resonance vibration increased threefold compared to the original bearing geometry. Additionally, a small increase was observed in the 3rd harmonic component. In contrast, the 2nd harmonic component decreased. The quadrangular case in Fig. 13 shows noise in harmonic response curves indicating a complicated excitation of the rotor.

In the vertical direction, the 4th harmonic resonance amplitude increased more than tenfold compared to the original bearing setup. In addition, a notable increase in the 3rd harmonic resonance peak was achieved. Instead, the 2nd harmonic resonance amplitude attenuated substantially leading to modest absolute amplitude values, which was seen as a small 2nd harmonic peak in Fig. 13 quadrangular case (vertical).

3.2.5. Bearing inner ring with minimized roundness error

In the horizontal direction, all the resonance peak amplitudes of the examined harmonic components decreased. The largest decrease of over 200 μm in comparison to the original bearing roundness profile was observed in the 2nd harmonic component. Since the 2nd harmonic component in horizontal direction was the major source of vibration in the original case, the decrease reduced the total vibration substantially as well.

In the vertical direction, the 2nd harmonic vibration peak amplitude decreased, although less than in the horizontal direction. With the original bearing roundness profile, the 2nd harmonic resonance peak amplitudes in horizontal and vertical direction differed substantially. With the minimized roundness error, the 2nd harmonic resonance amplitudes were observed to have the same magnitude in both directions. In addition the 4th harmonic component decreased slightly. However, despite the decrease in the 3rd waviness component in the bearing roundness profile (Fig. 12, triangular case), the 3rd harmonic resonance peak amplitude increased slightly.

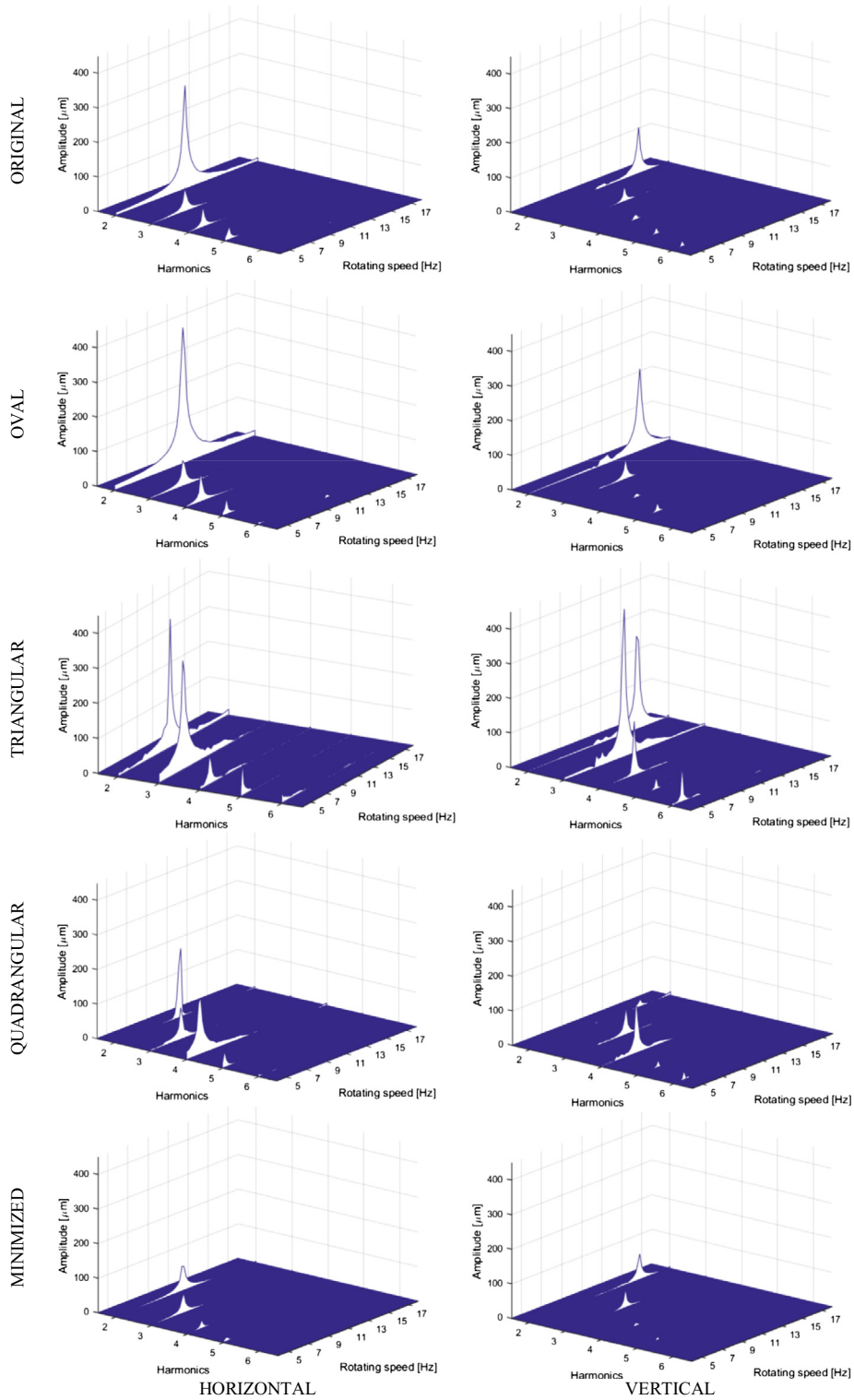


Fig. 13. Subcritical harmonic vibration components of the rotor at the middle cross-section (2000 mm) presented as a frequency spectrum in each bearing deformation case. Spectra are presenter separately for horizontal and vertical direction. The 1st harmonic vibration (eccentricity) is excluded from the study.

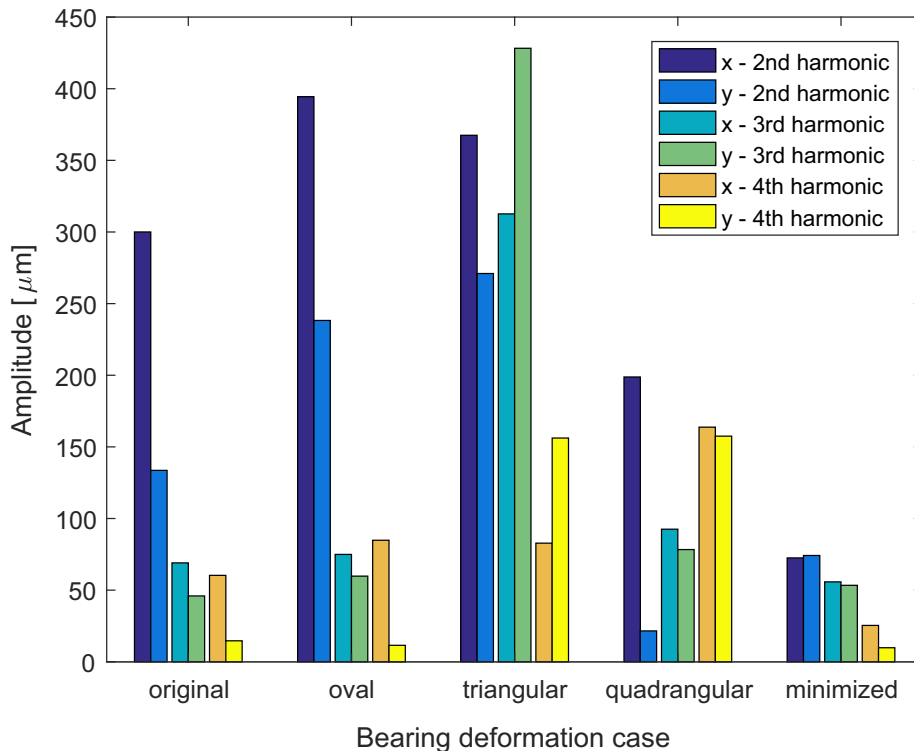


Fig. 14. The resonance peak amplitudes of subcritical harmonic vibrations in five different cases. Both horizontal (x) and vertical (y) direction amplitudes are presented.

4. Discussion

4.1. Relationships suggested by the results

In this study, the correlation between the geometry of the bearing inner ring and the large rotor subcritical vibration was investigated. Based on the measurement results, an obvious correlation exists.

The significant correlation between the bearing inner ring waviness component amplitudes and the peak amplitudes at the subcritical resonance frequencies of the rotor was observed. Generally, increasing the amplitude of a certain waviness component of the bearing roundness profile led to significantly increased corresponding subharmonic resonance amplitudes. The subcritical rotational frequency is found by dividing the natural frequency of the system by the waviness number in question.

Furthermore, the results clearly suggest that the rotor system had different natural frequencies in the vertical and horizontal directions. Based on the observed resonance frequencies, the natural frequency was c. 30 Hz in the vertical direction and c. 21.6 Hz in the horizontal direction. The dissimilar natural frequencies were very likely due to the asymmetric stiffness of the foundation, which was stiffer in the vertical direction compared to the horizontal.

Different natural frequencies revealed also another phenomenon, which is clearly observable in Fig. 13 (original and oval cases, vertical direction). The horizontal 2nd harmonic resonance had an effect on the vertical direction 2nd harmonic spectrum, which was observed as a small peak in the vertical direction 2nd harmonic response curve. The phenomenon may have been caused by the resonance vibration in one direction transmitted to the foundation, which in turn conveyed the excitation in another direction. In contrast, the resonances in the vertical direction had almost no observable effect on the horizontal direction vibration. The vibration amplitudes were in general greater in the horizontal direction due to a more flexible foundation, which may be the reason for the amplified vibrations in the vertical direction at horizontal direction resonance frequencies.

Notably differing natural frequencies in the horizontal and vertical directions led to one additional phenomenon: the 2nd harmonic resonance frequency in the horizontal direction (c. 10.8 Hz) was relatively close to the 3rd harmonic resonance frequency in the vertical direction (c. 10 Hz). A remarkable increase in the vertical 3rd harmonic vibration with the triangular bearing may result from the horizontal direction 2nd harmonic resonance excitation being approximately at the same frequency, considering the resonance vibration interplay explained above.

The final test case presented the results of the roll dynamic response with a tending side bearing inner ring, the roundness error of which was minimized. All the inspected lobe amplitudes of the inner ring roundness profile decreased substantially (Fig. 12). The decreases in the harmonic vibration resonance peaks (Fig. 14), although expected, were considerable, and clearly demonstrated the significance of the adjusted bearing inner ring roundness profile. Micrometre range variations in the inner ring roundness profile had a multiplied effect on the rotor dynamic behaviour and rotational accuracy in proximity to the harmonic frequencies.

4.2. Practical considerations

In practical engineering of large flexible rotors for example in paper machines, the typical design criteria aim to adjust the operating rotating frequency range below the half-critical speed (2nd H) [28], since the vibration problems caused by half-critical resonance are widely acknowledged. However, as proposed in the present study, 3rd harmonic and 4th harmonic resonances may exhibit significant amplitudes of vibration as well, and they may occur in the operational rotating frequency range limiting the usable speed range of the production and reducing the quality of the end product.

For example, in the field of paper manufacturing, from 10 to 100 μm amplitude level vibration (dynamic run-out) of the paper machine roll at operational rotating frequency causes significant coating (peak-to-peak c. 3 g/m^2), thickness (peak-to-peak c. 1.5 μm) and gloss (peak-to-peak 5%) variations in the paper, which are all important quality factors of the end product, and affect the printing process and printing quality substantially [2]. Consequently, the present study shows, that the bearing excitations from the bearing inner ring can cause noteworthy vibration problems (amplitudes hundreds of micrometers) in terms of required running accuracy in the field of paper production. Moreover, the study shows that by reducing the roundness error of the bearing inner ring, the vibration amplitudes reduced substantially.

In practical engineering and design of the rotors, this study reveals, that attention must be paid to the higher harmonic resonances, i.e., 3rd and 4th etc. and their root causes in addition to the traditionally noted half-critical (2nd H) resonance.

4.3. Measurement uncertainty

In the measurements, the emphasis was not on obtaining the most accurate estimates of the true value, but rather on discovering the changes and differences between the cases. Nevertheless, the measurement accuracies have been reflected in both dynamic and roundness profile measurement cases by Juhanko and Widmaier et al. [23,28]. Juhanko arrived finally at an expanded uncertainty of $U \leq 2 \mu\text{m}$ for the dynamic measurement device, whereas Widmaier et al. yielded an estimation from 1.5 μm to 2.5 μm for the tactile geometry measurement. Considering these accuracy limitations, the results remain valid and usable.

4.4. Comparison with previous research

The results presented in this paper show similar vibration behaviour as simulation results in the earlier published research, e.g., by Sopenan and Mikkola [18,19] and Heikkinen [21]. The bearing excitation frequency equations proposed by several authors are confirmed (Eqs. (1) and (2) in Section 1).

Various authors have developed several simulation models for the bearing excitation problem, as presented in Section 1. However, the simulation studies typically discuss only cases in which the inner ring waviness number is significantly higher than the waviness numbers in this study. The bearing size also is small which limits the number of bearing elements. The limited number of bearing elements leads to a situation in which the waviness numbers close to the number of elements produce the most important vibration excitations. In addition, the rotor mass in the earlier published bearing excitation studies has been substantially smaller, limiting the usefulness of the results in industrial purposes. Experimental results concerning bearing excitations in a rotor system have been limited. Measured results have typically been used for validation purposes of mathematical or simulation models. In addition, the measurements have been conducted using small laboratory-scale test devices. In contrast, this research utilized an industry-scale rotor system (paper machine roll) for measurements. Moreover, a proper series of measurements was conducted using different bearing inner ring roundness profiles as inputs.

4.5. Limitations and further research

In this study, only the tending side bearing geometry was varied. More research is needed to discover the interplay of the bearing excitations when the inner ring lobe amplitudes and their phases in both rotor ends are taken into account. For example, utilizing simulation models [18,19,21] may provide useful initial data for experimental research.

This study focused only on the low order waviness based excitations, since they more probably cause subcritical resonance vibration problems in the operating rotating frequency ranges of large rotors than higher order waviness. For example in paper machines, the rotating frequency ranges are typically from 10 Hz to 30 Hz. Large flexible rotors in this kind of applications tend to have the 1st bending mode natural frequency in the range of 20 Hz to 40 Hz. This leads to subcritical vibration resonances 2H (due to 2nd order waviness) at 10...20 Hz, 3H (due to 3rd order waviness) at 6.6...13.3 Hz and 4H (due to 4th order waviness) at 5...10 Hz. Consequently, the higher order waviness of the bearing inner ring causes subcritical

vibration resonance at lower frequency ranges, which is less problematic, because the typical operating frequencies are higher.

The roundness profile of the outer ring was excluded of the study as well. As in the present study, the outer ring is typically not rotating, and therefore it does not generate harmonic excitation to the rotor system. Moreover, the spherical roller bearing of a large rotor has a clearance between the rolling elements and the outer ring on the non-supporting side of the bearing. The clearance leads to a situation, where main part of the supporting force from the stationary outer ring to the roller elements is directed from one direction. In the present study, the clearance was on the upper side of the bearing since gravity was the only load. Consequently, the outer ring waviness effect is not synchronized with the rotating frequency of the rotor and the effect on subcritical resonances is be limited.

The roundness value of the inner ring changed between the cases. In the last case, the roundness error was intentionally reduced to enhance the rotating accuracy of the rotor. In addition, since the ovality (2nd order waviness) was already the dominating component in the original roundness profile, increasing the ovality led consequently to larger roundness error. As a downside, the value of the roundness error could not be maintained. The waviness components could not be manipulated in a mathematically accurate way, which would have been possible in a simulation approach, since the study was experimental. Although the roundness error varies in different cases, the authors consider, that changing the amplitudes of the low order waviness components and comparing their effect on harmonic components of subcritical vibration is essential in this paper.

The method to deform the inner ring by inserting thin steel strips between the rotor shaft and the conical adapter sleeve could be considered as one method to achieve minimized roundness errors of assembled bearing inner rings. However, the steel strips may deform the rotor shaft or move during the operation, particularly if the rotor is heavily loaded, leading to a loss of benefits. The wide use of the steel strip method requires a profound test series under varying loads and continuous operation for a long time span if considering, for example, an application in the paper industry.

Instead of inserting steel strips between the rotor shaft and the conical adapter sleeve, the rotor shaft could be ground to a roundness profile, which minimizes the final roundness error of the assembled bearing inner ring. In the designs without the conical adapter sleeve, the cone could be ground directly on the rotor shaft with a roundness profile, which minimizes the final roundness error of the bearing inner ring as well. For non-circular precision grinding purposes, the 3D grinding method can be used [2]. This method would decrease the uncertainties related to the steel strips discussed in the previous paragraph.

Furthermore, one option is to reduce the thickness variation of the bearing inner ring and of the possible conical sleeve. Based on the results of this research, the bearing manufacturers should especially concentrate on minimizing the thickness variation of the bearing inner ring and the possible conical adapter sleeve instead of the roundnesses of the individual elements. The roundness of a separate inner ring is irrelevant, as the inner ring is tightened to a stiffer shaft having a roundness profile of its own. If the thickness variation is minimized, the rotor manufacturer could concentrate on the machining of a round rotor shaft. Research considering the individual element precision (bearing inner ring, conical adapter sleeve and rotor shaft) is needed to recognize the root causes for bearing based excitation of rotors.

Acknowledgements

The authors would like to thank Dr. Vesa Saikko for his valuable effort in reviewing this article.

Funding

This work was supported by Academy of Finland (ViDROM, grant number 277964) and EMRP (DriveTrain, grant number ENG56-REG1).

Declaration of interest

The authors have nothing to declare.

References

- [1] C.M. Harris, A.G. Piersol, *Harris' Shock and Vibration Handbook*, McGraw-Hill, New York, 2002.
- [2] P. Kuosmanen, Predictive 3D Roll Grinding Method for Reducing Paper Quality Variations in Coating Machines, Helsinki University of Technology, 2004.
- [3] O.G. Gustafsson et al., Research report on study of the vibration characteristics of bearings, Research Laboratory SKF industries, 1963.
- [4] E.M. Yhland, *Waviness measurement-an instrument for quality control in rolling bearing industry*, *Proc. Inst. Mech. Eng.* 182 (1967) 438–445.
- [5] A.H. Slocum, *Precision Machine Design*, Prentice Hall, New Jersey, 1992.
- [6] N. Aktürk, The effect of waviness on vibrations associated with ball bearings, *J. Tribol.* 121 (1999) 667–677, <https://doi.org/10.1115/1.2834121>.
- [7] H. Arslan, N. Aktürk, An investigation of rolling element vibrations caused by local defects, *J. Tribol.* 130 (2008) 41101, <https://doi.org/10.1115/1.2958070>.
- [8] B. Changqing, X. Qingyu, Dynamic model of ball bearings with internal clearance and waviness, *J. Sound Vib.* 294 (2006) 23–48, <https://doi.org/10.1016/j.jsv.2005.10.005>.
- [9] S.P. Harsha, K. Sandeep, R. Prakash, The effect of speed of balanced rotor on nonlinear vibrations associated with ball bearings, *Int. J. Mech. Sci.* 45 (2003) 725–740, [https://doi.org/10.1016/S0020-7403\(03\)00064-X](https://doi.org/10.1016/S0020-7403(03)00064-X).

- [10] S.P. Harsha, K. Sandeep, R. Prakash, Non-linear dynamic behaviors of rolling element bearings due to surface waviness, *J. Sound Vib.* 272 (2004) 557–580, [https://doi.org/10.1016/S0022-460X\(03\)00384-5](https://doi.org/10.1016/S0022-460X(03)00384-5).
- [11] S.P.P. Harsha, P.K.K. Kankar, Stability analysis of a rotor bearing system due to surface waviness and number of balls, *Int. J. Mech. Sci.* 46 (2004) 1057–1081, <https://doi.org/10.1016/j.ijmecsci.2004.07.007>.
- [12] S.P. Harsha, Rolling bearing vibrations – the effects of surface waviness and radial internal clearance, *Mech. Eng.* (2006) 91–111, <https://doi.org/10.1080/155022891010015>.
- [13] S.P. Harsha, Nonlinear dynamic analysis of a high-speed rotor supported by rolling element bearings, *J. Sound Vib.* 290 (2006) 65–100, <https://doi.org/10.1016/j.jsv.2005.03.008>.
- [14] G.H. Jang, S.W. Jeong, Nonlinear excitation model of ball bearing waviness in a rigid rotor supported by two or more ball bearings considering five degrees of freedom, *J. Tribol. ASME*. 124 (2002) 82–90, <https://doi.org/10.1115/1.1398289>.
- [15] C.K. Babu, N. Tandon, R.K. Pandey, Nonlinear vibration analysis of an elastic rotor supported on angular contact ball bearings considering six degrees of freedom and waviness on balls and races, *J. Vib. Acoust.* 136 (2014) 44503, <https://doi.org/10.1115/1.4027712>.
- [16] D.S. Shah, V.N. Patel, Study on excitation forces generated by defective races of rolling bearing, *Procedia Technol.* 23 (2016) 209–216, <https://doi.org/10.1016/j.protcy.2016.03.019>.
- [17] W. Liu, Y. Zhang, Z.J. Feng, J.S. Zhao, D. Wang, A study on waviness induced vibration of ball bearings based on signal coherence theory, *J. Sound Vib.* 333 (2014) 6107–6120, <https://doi.org/10.1016/j.jsv.2014.06.040>.
- [18] J. Sapanen, A. Mikkola, Dynamic model of a deep-groove ball bearing including localized and distributed defects. Part 1: theory, *Proc. Inst. Mech. Eng. Part K J. Multi-Body Dyn.* 217 (2005) 201–211. <http://doi.org/10.1243/14644190360713560>.
- [19] J. Sapanen, A. Mikkola, Dynamic model of a deep-groove ball bearing including localized and distributed defects. Part 2: implementation and results, *Proc. Inst. Mech. Eng. Part K J. Multi-Body Dyn.* 217 (2005) 213–223. <http://doi.org/10.1243/14644190360713560>.
- [20] B. Ghalamchi, J. Sapanen, A. Mikkola, Dynamic model of spherical roller bearing, *Proc. ASME Des. Eng. Tech. Conf.* 8 (2013), <https://doi.org/10.1115/DETC2013-12970>.
- [21] J. Heikkinen, Vibrations in Rotating Machinery Arising From Minor Imperfections in component geometries, Lappeenranta University of Technology, 2014.
- [22] J. Heikkinen, B. Ghalamchi, R. Viitala, J. Sapanen, J. Juhanko, A. Mikkola, P. Kuosmanen, Vibration analysis of paper machine's asymmetric tube roll supported by spherical roller bearings, *Mech. Syst. Signal Process.* 104 (2018) 688–704, <https://doi.org/10.1016/j.ymsp.2017.11.030>.
- [23] T. Widmaier, B. Hemming, J. Juhanko, P. Kuosmanen, V.-P. Esala, A. Lassila, P. Laukkanen, J. Haikio, Application of Monte Carlo simulation for estimation of uncertainty of four-point roundness measurements of rolls, *Precis. Eng.* 48 (2017) 181–190, <https://doi.org/10.1016/j.precisioneng.2016.12.001>.
- [24] P.D. McFadden, A revised model for the extraction of periodic waveforms by time domain averaging, *Mech. Syst. Signal Process.* 1 (1987) 83–95, [https://doi.org/10.1016/0888-3270\(87\)90085-9](https://doi.org/10.1016/0888-3270(87)90085-9).
- [25] S. Braun, The synchronous (time domain) average revisited, *Mech. Syst. Signal Process.* 25 (2011) 1087–1102, <https://doi.org/10.1016/j.ymsp.2010.07.016>.
- [26] P.D. McFadden, M.M. Toozhy, Application of synchronous averaging to vibration monitoring of rolling element bearings, *Mech. Syst. Signal Process.* 14 (2000) 891–906, <https://doi.org/10.1006/mssp.2000.1290>.
- [27] D. Hochmann, M. Sadok, Theory of synchronous averaging, in: *IEEE Aerosp. Conf. Proc.*, 2004: pp. 3636–3653. <http://doi.org/10.1109/AERO.2004.1368181>.
- [28] J. Juhanko, Dynamic Geometry of a Rotating Paper Machine Roll, Aalto University, 2011.
- [29] S. Ozono, On a new method of roundness measurement on the three point method, in: *Proceedings of the ICPE, Tokyo, 1974*, pp. 457–462.